Journal of Experimental Botany, Vol. 63, No. 7, pp. 2787–2798, 2012
doi:10.1093/jxb/err465 Advance Access publication 20 January, 2012
This paper is available online free of all access charges (see http://jxb.oxfordjournals.org/open_access.html for further details)

Journal of Experimental Botany
www.jxb.oxfordjournals.org

RESEARCH PAPER

HYL1 controls the miR156-mediated juvenile phase of vegetative growth

Shuxia Li, Xi Yang, Feijie Wu and Yuke He*

National Key Laboratory of Plant Molecular Genetics, Shanghai Institute of Plant Physiology and Ecology, Shanghai Institutes for Biological Sciences, Chinese Academy of Sciences, Fenglin Road 300, Shanghai 200032, China

* To whom correspondence should be addressed. E-mail: ykhe@sibs.ac.cn

Received 13 October 2011; Revised 23 December 2011; Accepted 27 December 2011

Abstract

HYL1 is an important regulator of microRNA (miRNA) biogenesis. A loss-of-function mutation of *HYL1* causes the reduced accumulation of some miRNAs but fails to display the miRNA-deficient phenotypes of these miRNAs. In *Arabidopsis*, miR156 mediates phase transition through repression of *SQUAMOSA PROMOTER-BINDING PROTEIN-LIKE* (*SPL*) genes. However, it remains unknown whether, and if so how, HYL1 enables phase transition through miR156. This study showed that a loss-of-function mutation of the *HYL1* gene caused defects in the timing of the juvenile phase. In the primary leaves of *hyl1-2* mutants, abaxial trichomes were generated prematurely, the leaf blades elongated, and the blade base angles enlarged, as is observed for adult leaves. In *hyl1-2 p35S::miR156a* and *hyl1-2 spl9-4 spl15-1* plants, increased accumulation of miR156a and repressed expression of the *SPL* genes were concomitant with a complete or partial rescue of the *hyl1-2* phenotype in phase defects. In contrast, overexpression of the *SPL9* gene in *hyl1-2* mutants led to total disappearance of the juvenile phase. Moreover, HYL1 prevented the premature accumulation of adult-related transcripts in the primary leaves. Taken together, these results suggest that HYL1 controls the expression levels of miR156-targeted *SPL* genes and enables plants to undergo the juvenile phase, an important and critical step during plant development to ensure maximum growth and productivity.

Key words: HYL1, juvenile phase, miR156, *SPL9*, vegetative growth.

Introduction

Plants undergo several developmental transitions, including the transition from an embryonic to post-embryonic mode of growth, the juvenile-to-adult vegetative transition, and the vegetative-to-reproductive transition. The juvenile phase is an important and critical step during plant development to ensure maximum growth and productivity. The juvenile-to-adult-phase transition (vegetative change) usually involves changes in a variety of species-specific traits, including leaf shape, presence of trichomes and thorns, production of phytochemicals, leaf retention, internode length, and disease and pest resistance (Willmann and Poethig, 2011). The timing of the transition from the juvenile to the adult phase is significantly influenced by environmental cues, such as day length, light intensity, ambient temperature, and the plant hormone gibberellic acid (Willmann and Poethig, 2005). However, this transition is also controlled genetically. Recently, genetic analyses of developmental maturation in plants have advanced significantly, and some of the genetic elements involved in phase transition have been identified.

One of these identified genetic elements is the microRNA (miRNA) miR156, which is highly expressed early in shoot development and decreases with time. Overexpression of miR156 prolongs the juvenile-phase length and delays flowering (Wu and Poethig, 2006; Chuck *et al.*, 2007; Wang *et al.*, 2009). miR156 targets the SQUAMOSA PROMOTER BINDING-LIKE (SPL) transcription factors, which influence developmental transitions. In *Arabidopsis thaliana*, there are 16 members of the SPL family of transcription factors. Ten of the miR156-targeted *SPL*

Abbreviations: BBA, blade base angle; miRNA, microRNA; pri-miRNA, primary transcript miRNA.

genes are grouped into different clades: *SPL3*/*SPL4*/*SPL5*, *SPL2*/*SPL10*/*SPL11*, *SPL6*/*SPL13* and *SPL9*/*SPL15* (Guo *et al.*, 2008).The first clade consists of *SPL3*, *SPL4*, and *SPL5*, which encode small proteins that contain a SQUAMOSA promoter DNA-binding protein domain. Constitutive overexpression of *SPL3*, *SPL4*, or *SPL5* accelerates the juvenile-to-adult-phase change and advances flowering time (Wu and Poethig, 2006), whereas overexpression of *SPL9* and its closely related paralogue *SPL15* not only shortens the juvenile phase and produces an early flowering phenotype but also affects changes in the cell size and cell number typical of adult leaves (Usami *et al.*, 2009). In addition, the gain-of-function phenotype of *SPL10* or its closely related paralogues *SPL2* and *SPL11* also affects leaf initiation and developmental transitions (Shikata *et al.*, 2009). Although it is well known that the juvenile-to-adult transition depends on the accumulation of miR156 (Chuck *et al.*, 2007; Wang *et al.*, 2008; Wu *et al.*, 2009), the upstream elements that determine the temporal and spatial expression patterns of miR156 remain unclear.

The processing of miRNAs from longer primary transcripts (pri-miRNAs) requires the activity of several proteins, including DICER-LIKE1 (DCL1), the double-stranded RNA-binding protein HYPONASTIC LEAVES1 (HYL1), and the zinc-finger protein SERRATE (SE) (Hiraguri *et al.*, 2005; Kurihara *et al.*, 2006; Lobbes *et al.*, 2006; Dong *et al.*, 2008; Yang *et al.*, 2010; Machida *et al.*, 2011). All three proteins are found in nuclear processing centres called D-bodies (Fang and Spector, 2007; Fujioka *et al.*, 2007; Song *et al.*, 2007). Mutants deficient in miRNA biogenesis exhibit increased pri-miRNA levels and reduced amounts of mature miRNAs, and suffer from a wide range of morphological defects (Han *et al.*, 2004; Vazquez *et al.*, 2004; Lobbes *et al.*, 2006; Yang *et al.*, 2006). The loss-of-function mutants *hyl1* and *hyl1-2*, which are disrupted by Ds and T-DNA insertions, respectively, display a series of mutant phenotypes such as shorter stature, narrower hyponastic leaves, delayed flowering, and reduced fertility (Lu and Fedoroff, 2000; Vazquez *et al.*, 2004).

Changes in the transition from the juvenile to the adult phase are reported in loss-of-function mutants of *SE* (Clarke *et al.*, 1999). Similarly, a mutation in a recessive allele of *ARGONAUTE1* (*AGO1*), which encodes the enzyme responsible for cleavage of miRNA transcripts in *Arabidopsis*, significantly affects leaf initiation in plants (Wang *et al.*, 2008). However, it remains unknown whether the juvenile-to-adult-phase transition is affected in *hyl1* mutants. Many miRNAs act by silencing their target genes, and deregulation of these miRNAs usually produces morphological changes. However, deregulation of some miRNAs that occur in *hyl1* mutants does not lead to obvious phenotypes (Liu *et al.*, 2011). The morphological interaction between HYL1-regulated miRNA biogenesis and miRNA-mediated gene silencing is complicated. To answer whether, and if so how, HYL1 controls the miR156-regulated phase transition, we conducted a genetic and molecular analysis of *HYL1*, as well as miR156 and its targets. The results indicated that HYL1 functions as an upstream regulator of miR156 in maintenance of the juvenile phase.

Materials and methods

Plant material and growth conditions

The wild-type and mutant *A. thaliana* plants used in this study were of the Columbia ecotype (Col-0), unless otherwise indicated. The plasmids *pSPL9::rSPL9* and *pSPL10::rSPL10* were gifts from Dr R. Scott Poethig (University of Pennsylvania, PA, USA), and plasmid *p35S::rSPL3* was a gift from Dr Detlef Weigel (The Salk Institute for Biological Sciences, CA, USA).

Seeds were sown and grown at 22 °C under long (16 h light/8 h dark) and short (8 h light/16 h dark) day conditions. *hyl1-2* mutant T-DNA insertion lines were obtained from the Arabidopsis Biological Resource Center (OH, USA). The *spl9-4 spl15-1* mutant was a gift from Dr Scott Poethig (Wu *et al.*, 2009). Seeds were surface sterilized in 70% ethanol for 1 min, followed by 0.1% $HgCl_2$ for 10 min, and then washed four times in sterile distilled water and plated in molten 0.1% agar in water on top of solid 1% sugar MS0 medium. The plates were sealed with Parafilm, incubated at 4 °C in the dark for 2–3 d, and then moved to a growth chamber at 22 °C with 8 h light (short day).

For phenotypic observations, the seeds were sown in pots with peat soil and grown in a growth chamber under the same conditions. The blade width, blade length, and petiole length were measured. For leaf-shape analysis, fully expanded leaves were removed, attached to A4 paper with double-sided tape, flattened, and measured using vernier calipers. The abaxial trichomes were scored 60 d after planting, using a stereomicroscope.

Transgenic plants

Fragments corresponding to precursor of miR156a were inserted into pCAMBIA3301 binary vectors and placed under the control of the cauliflower mosaic virus 35S promoter. The binary constructs were delivered into *Agrobacterium tumefaciens* strain GV3101 (pMP90RK) using a freeze–thaw method (Weigel and Glazebrook, 2006). The *Arabidopsis* plants were transformed using a flower-dip method (Clough and Bent, 1998). For selection of transgenic plants, the seeds were sterilized and germinated on agar medium containing 50 mg l^{-1} kanamycin and 10 mg l^{-1} phosphinothricin. Seedlings conferring resistance to the herbicide Basta or to kanamycin were transplanted in a greenhouse and grown at 22 °C under an 8 h light regime. The transgenic plants were selfed for at least three generations, and the seeds from each plant were harvested separately for subsequent observations.

Small-RNA deep sequencing

All *hyl1* plants were grown under a 16 h light/8 h dark photoperiod at 22 °C for 3 weeks. RNA samples from the aboveground parts of the seedlings were prepared using the Illumina Alternative v1.5 Protocol, and small-RNA deep sequencing was performed using an Illumina GAII sequencer and the mirVana™ miRNA Isolation Kit (Ambion).

Real-time PCR

Total RNA was extracted with TRIzol (Invitrogen) and treated with DNase I (Takara) to remove DNA contamination. Approximately 4 μg RNA was used for reverse transcription with oligo(dT) primers. Real-time PCR was performed using specific pairs of primers (see Supplementary Table S3, available in *JXB* online. The comparative threshold cycle (C_t) method was used to determine relative transcript levels in the real-time PCR (MyiQ2 Two-color Real-time PCR Detection System; Bio-Rad). Three biological replicates and three technical replicates were performed.

In situ *hybridization*

HYL1 full-length coding sequence was PCR amplified and cloned into pBluescript SK. Digoxigenin-labelled sense and antisense probes were synthesized with T7 or T3 RNA polymerase (Takara). For the miR156a probe, locked nucleic acid-modified probes of miR156a were synthesized and labelled with digoxigenin at the 3′ end by TaKaRa and used for *in situ* hybridization. Shoot apices from 20-d-old short-day-grown wild-type plants were prepared following pre-treatment and hybridization methods described previously (Liu *et al.*, 2011).

Northern blotting

A volume containing 30–50 μg RNA was separated on 19% polyacrylamide denaturing gels. The RNA was transferred to a Hybond membrane (Amersham Biosciences, GE Healthcare) for 2 h at 200 mA. After cross-linking by UV irradiation for 3 min, the Hybond membrane was hybridized with biotin-labelled DNA probes complementary to the predicted miRNA sequences at 42 °C overnight. The membrane was washed at 42 °C twice with 2× SSC and 0.1% SDS, followed by two higher stringency washes of 0.1× SSC and 0.1% SDS at 42 °C. Subsequently, the membrane was incubated with a stabilized streptavidin–horseradish peroxidase conjugate (Thermo Scientific) in nucleic acid detection blocking buffer and then washed five times with 1× washing buffer. After washing with substrate equilibration buffer and adding stable peroxide solution and enhancer solution, the blots were imaged using an FLA-5000 Phosphorimager (FujiFilm). To confirm uniform loading, the blots were also probed with a DNA probe complementary to the U6 gene as a control. The DNA probes used for small-RNA northern blotting were synthesized and biotin-labelled using a 3′-end DNA labelling method (Invitrogen).

Microarray analysis

The *hyl1-2* and Nossen ecotype seedlings were grouped randomly and grown under identical conditions for 3 weeks. Each group contained five seedlings and was designated as one biological replicate. Six biological replicates for each plant line were prepared, and three were used for array experiments.

GeneChip array analysis was performed using Affymetrix ATH1 microarrays (ATH1 121501). Differentially expressed genes were identified from expression data acquired from six independent microarray hybridizations. Three replicates of *hyl1* RNA and wild-type reference RNA were used to calculate the expression values for each gene. For analysis of the expression profile, the fold changes in the normalized signals derived from three *hyl1* replicates and three wild-type replicates were calculated. Only the fold changes of genes that met a significance criterion of $P < 0.05$ with a fold change of >1.5 are presented.

Results

HYL1 maintains the juvenile phase of primary leaves

hyl1 mutants are deficient in miRNA processing and exhibit pleiotropic abnormalities that include a shorter stature and hyponastic leaves (Lu and Fedoroff, 2000). *hyl1-2* is a hypomorphic allele of *hyl1*, and both share the same mutant phenotypes. Under short-day conditions, the vegetative period of *hyl1-2* mutants was shortened compared with the wild type, and all of the rosette leaves curved upward, making it difficult to observe transition from the juvenile to the adult phase (Fig. 1A, B). To examine whether mutation of the *HYL1* gene altered vegetative phase transition, we carried out phenotyping of the *hyl1-2* plants under short-day conditions. In wild-type plants, abaxial trichomes were not observed on the first nine leaves but became evident on the 13th leaves and progressively numerous on the 15th leaves and thereafter (Fig. 2A). According to the timing of abaxial trichomes, the first nine leaves were juvenile and the 13th and subsequent leaves were adult (Fig. 1C). Among these leaves, the first two leaves (primary leaves) and third leaves were representative of the early juvenile phase, and the 13th to 15th leaves were representative of the adult phase, and thus we paid particular attention to the first three leaves and the 13th to 15th leaves. Compared with wild-type plants, the juvenile phase of the *hyl1-2* plants was defective. Abaxial trichomes were observed on most of the primary leaves and on all of the third leaves of *hyl1-2* plants (Fig. 2A). Precisely, the abaxial trichomes on *hyl1-2* leaves were produced earlier than those in wild-type plants by 12 plastochrons. These observations demonstrated that the primary leaves of *hyl1-2* plants had acquired adult characteristics. In addition, the leaf shape index (length-to-width ratio) of the third leaf of the *hyl1-2* mutants resembled that of the 13th wild-type leaves. Due to their increased length, the *hyl1-2* blades appeared narrow and elongated. Moreover, the leaf initiation rate of the mutant plants was lower than that of wild-type plants (Fig. 1D). Taken together, these results showed that most of the primary leaves in *hyl1-2* plants were transformed from juvenile to adult leaves.

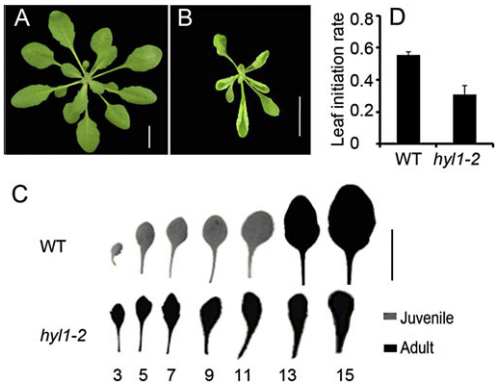

Fig. 1. Early phase transition of *hyl1-2* mutants. (A, B) Wild-type (A; WT) and *hyl1-2* (B) seedlings 30 d after germination (DAG). (C) Fully expanded leaves showing the leaf shape. Black leaves represent the adult phase, while grey leaves represent the juvenile phase; the numbers beneath are the leaf order counting from the primary leaves (the first two rosette leaves). Bar, 1 cm. (D) Leaf initiation rate (calculated by the formula: number of leaves initiated per plant/DAG) of *hyl1-2* 30-d-old plants. The number of plants observed was >30. Results are shown as means ±SD.

HYL1 determines the temporal and spatial accumulation of miR156 in the juvenile phase

HYL1 is one of the major regulators of miRNAs in plants. To verify the function of HYL1 in the production of miR156 and other related miRNAs, we examined the

abundance of small RNAs in *hyl1* and wild-type seedlings (Nossen ecotype) by small-RNA deep sequencing. This high-throughput sequencing identified a total of 5.3 million and 6.2 million small RNA sequences from samples from *hyl1* and wild-type seedlings, respectively. We normalized each dataset of small RNAs to transcripts per 5 million and observed that the *hyl1* and wild-type datasets contained 61 and 77 miRNAs, respectively, that are conserved in *Arabidopsis*. The expression of most of these miRNAs was downregulated in the *hyl1* seedlings compared with the wild-type (>1.5-fold), and among them, miR156a–f were the most downregulated (>10-fold) (Table 1). As miR156 and miR157 target *SPL* genes, we focused on differences in the expression of members of the miR156 family. The mature sequences of miR156g and miR156h presented several mismatches with miR156a, and these miRNAs were regulated differentially by *HYL1*. The expression of miR156g was downregulated 3.5-fold in the *hyl1* seedlings. In contrast to miR156a and miR156g, expression of miR156h was not downregulated in the *hyl1* seedlings. Nevertheless, miR156h was less abundant than miR156a in both the wild-type and *hyl1* seedlings. As expected, miR157a–c and miR157f were downregulated in the *hyl1* seedlings. Differential abundance of miR156 members might result in different silencing of the target genes. However, the total accumulation of miR156 in *hyl1* seedlings was much lower than in the wild type.

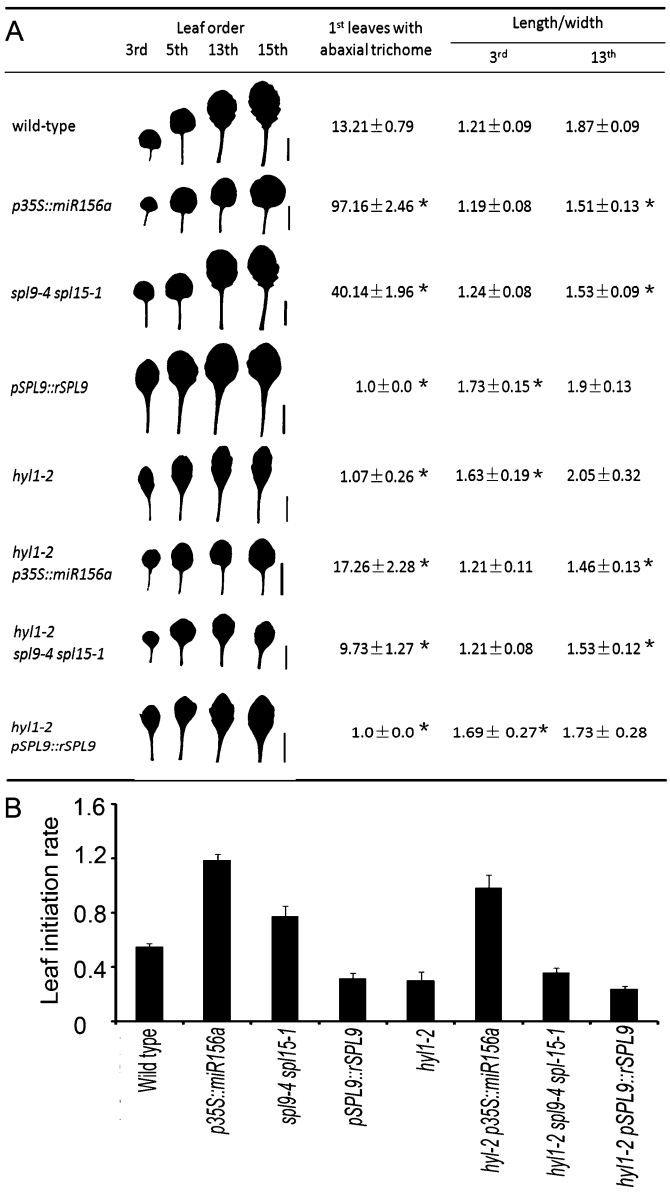

Fig. 2. Parameters of *hyl1-2* and transgenic plants, and triple mutants. (A) Leaf shape, abaxial trichomes, and leaf length-to-width ratios of *hyl1-2* and related plants. Bars, 1 cm. (B) Leaf initiation rate of *hyl1-2*, *hyl1-2 p35S::miR156a*, and *hyl1-2 pSPL9::rSPL9* plants (n=30). Asterisks indicate significant differences from the wild type (P <0.01) and results are shown as means ±SD.

The vegetative-phase transition depends on the accumulation of miR156 and temporal changes in the expression of miR156-targeted *SPL* genes (Wu *et al.*, 2009). If HYL1 controls the expression of miR156, the spatial and temporal patterns of miR156 should be correlated with those of *HYL1*. To address this point, we performed *in situ* hybridization and quantitative real-time PCR analyses of the *HYL1* gene. The *HYL1* gene was expressed preferentially in the shoot apical meristem, leaf primordial, and growing leaves (Fig. 3A, B). Real-time PCR revealed that *HYL1* expression increased rapidly in 7–13-d-old seedlings and was maintained at relatively high levels from d 13 to 19 (Fig. 3D). *In situ* hybridization showed that miR156a accumulated in the same regions as *HYL1* expression, except that stronger accumulation was observed in the shoot apical meristem (Fig. 3C). To confirm whether the accumulation of miR156a was upregulated during the vegetative phase, we harvested the shoot apices of *hyl1-2* plants, and used small-RNA northern blotting to detect the

Table 1. Down- and upregulation of miRNAs in *hyl1* seedlings relative to the wild type

	miRNA	Sequence	Reads		*hyl1*/WT
			WT	*hyl1*	
Ten miRNAs most deregulated					
1	miR156a–f	TGACAGAAGAGAGTGAGCAC	129 754	12 776	0.098
2	miR158a	TCCCAAATGTAGACAAAGCA	91 804	30 001	0.327
3	miR167	TGAAGCTGCCAGCATGATCTA	29 246	24 066	0.403
4	miR166a–g	TCGGACCAGGCTTCATTCCCC	5 736	2 312	0.403
5	miR157d	TGACAGAAGATAGAGAGCAC	3 733	2 237	0.599
6	miR843a	TTTAGGTCGAGCTTCATTGGA	3 474	1 451	0.418
7	miR161a.2	TTGAAAGTGACTACATCGGGG	2 587	552	0.213
8	miR168	TCGCTTGGTGCAGGTCGGGAA	2 360	6 312	2.675
9	miR396b	GCTCAAGAAAGCTGTGGGAAA	2 291	761	0.332
10	miR172a–b	AGAATCTTGATGATGCTGCAT	2 123	2 514	1.184
Different types of miR156 and miR157					
1	miR156a–f	TGACAGAAGAGAGTGAGCAC	129 754	12 776	0.098
2	miR156g	CGACAGAAGAGAGTGAGCAC	145	42	0.290
3	miR156h	TGACAGAAGAAAGAGAGCAC	10	11	1.100
4	miR157a–c	TTGACAGAAGATAGAGAGCAC	76 378	57 268	0.750
5	miR157d	TGACAGAAGATAGAGAGCAC	3 733	22.37	0.599

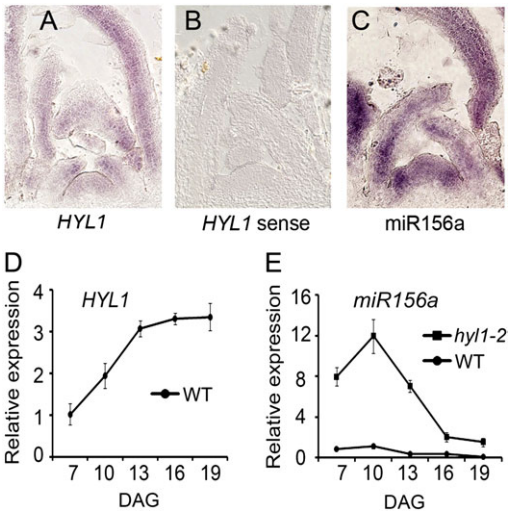

Fig. 3. Expression pattern of *HYL1* and pri-miR156a. (A–C) RNA *in situ* hybridization of *HYL1* with antisense (A) and sense (B) probes and miR156a (C), showing spatial expression of *HYL1* and miR156a in the shoot tips of *Arabidopsis* seedlings at 3 weeks grown under short-day conditions. (D) Temporal expression pattern of *HYL1*. (E) Temporal expression pattern of pri-miR156a. Three biological replicates were performed. DAG, Days after germination; WT, wild type. Results are shown as means ±SD.

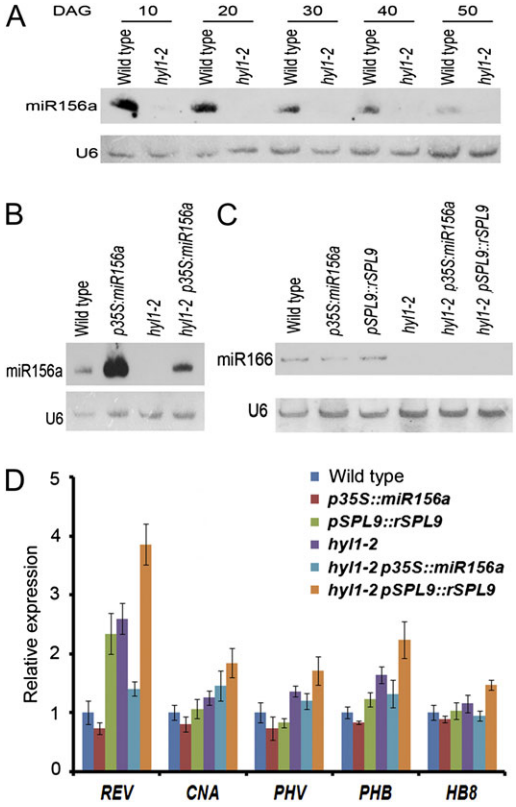

Fig. 4. Expression of miR156, miR165/6 and HD-ZIP III. (A, B) Northern hybridization showing the accumulation of miR156a in shoot apices of *hyl1-2* plants at different stages (10–50 d after germination (DAG)) (A), and of *hyl1-2 p35S::miR156a* plants at 20 DAG (B). (C) Northern hybridization showing the accumulation of miR165/6 in shoot apices of *hyl1-2 p35S::miR156a* and *hyl1-2 pSPL9::rSPL9* plants at 10 DAG. U6 was used as a control. (D) Expression levels of HD-ZIP III genes in *hyl1-2 p35S::miR156a* and *hyl1-2 pSPL9::rSPL9* plants at 10 DAG. Three biological replicates were performed.

accumulation of miR156a at various stages (10-, 20-, 30-, 40-, and 50-d-old seedlings). In wild-type plants, the levels of miR156a accumulation were highest at 10 d of age and subsequently declined over time. Similarly, the accumulation of miR156a in *hyl1-2* seedlings decreased from 10 to 20 d. However, the accumulation of miR156a in *hyl1-2* seedlings was much lower than that of the wild type at d 10, and almost undetectable from d 20 (Fig. 4A).

It was possible that the reduced accumulation of miR156a in *hyl1-2* mutants was dependent on the amount of pri-miR156a. To exclude this possibility, we analysed the amount of pri-miR156a in shoot apices of both wild-type and *hyl1-2* plants using reverse transcription followed by real-time PCR. During the vegetative phase, the level of pri-miR156a in *hyl1-2* seedlings was greater than that of the wild type, in contrast to the accumulation of miR156a (Fig. 3E). This was consistent with a previous report (Kurihara *et al.*, 2009). Like the wild type, the transcript level degreased progressively from d 10 to 19 in *hyl1-2* seedlings. In the primary leaves of *hyl1-2* mutants, reduced accumulation of miR156a and increased levels of pri-miR156a were coincident with adult characteristics, indicating that HYL1 might control the accumulation of miR156 by post-transcriptional regulation rather than by transcriptional regulation.

If HYL1 promotes juvenile epidermal identity, increased accumulation of miR156 should rescue the epidermal defects seen in *hyl1-2* mutants. To define the genetic interaction between *HYL1* and miR156, we created *hyl1-2* transgenic plants that accumulated miR156 under the control of a constitutive cauliflower mosaic virus 35S promoter (Fig. 5A, B, D and E). Wild-type plants transformed with *p35S::miR156a* presented a prolonged juvenile epidermal phenotype. Introduction of *p35S::miR156a* into *hyl1-2* plants completely rescued the epidermal defects (Fig. 2A). Compared with *hyl1-2* plants, *hyl1-2 p35S::miR156a* exhibited delayed production of abaxial trichomes by 16.2 plastochrons, which was almost what was seen in wild-type plants. Consistent with the rescue of the epidermal defects, the leaf initiation rate increased 1.5-fold relative to that of the wild type (Fig. 2B), and the juvenile leaf blades were rounded, similar to the wild type (Fig. 5G). To address whether there was overproduction of miR156a in *hyl1-2 p35S::miR156a* plants, we examined the accumulation of miR156a in 10-d-old seedlings by northern blotting. The accumulation of miR156a was enhanced in *hyl1-2 p35S::miR156a* seedlings relative to *hyl1-2* and wild-type plants but did not overaccumulate as in the *p35S::miR156a* seedlings (Fig 4B). This indicated that the regulation of miR156a biogenesis by HYL1 was dose dependent. In this case, the abundance of miR156a in *hyl1-2 p35S::miR156a*

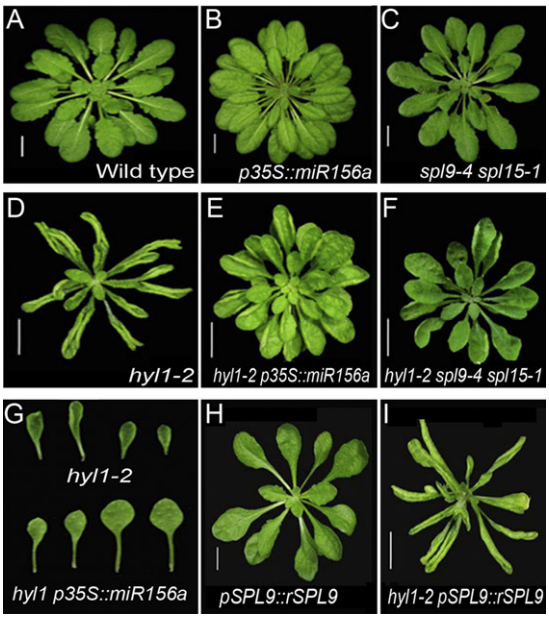

Fig. 5. Genetic interaction between *HYL1*, miR156a and *SPL* genes. (A–F) 60-d-old rosette seedlings of the wild-type (A), *p35S::miR156a* (B), *spl9-4 spl15-1* (C), *hyl1-2* (D), *hyl1-2 p35S::miR156a* (E) and *hyl1-2 spl9-4 spl15-1* (F) plants, grown under short-day conditions. (G) Individual leaves of *hyl1-2* and *hyl1-2 p35S::miR156a* plants. (H, I) Rosette seedlings (60-d-old) of *pSPL9::rSPL9* (H) and *hyl1-2 pSPL9::rSPL9* (I), grown under short-day conditions.

seedlings was high enough and over the threshold required for the juvenile phase. We suggest that HYL1 maintains the juvenile state of primary leaves through temporal and spatial regulation of miR156.

HYL1 controls the expression levels of miR156-targeted SPL *genes*

To define the expression levels of miR156-targeted genes in *hyl1* mutants, we applied ATH1 Affymetrix arrays to detect the global expression of miRNA-targeted genes. Among 22 810 genes, 657 genes were upregulated and 1247 genes were downregulated >1.5-fold in the *hyl1* seedlings. Among the 657 upregulated genes, there were 35 target genes for miRNAs and/or *trans*-acting small interfering RNAs, which accounted for 3.6% of the upregulated genes (Table 2). Among the ten members of the miR156-targeted *SPL* genes, *SPL3*, *SPL4*, *SPL5*, *SPL9*, and *SPL10* were upregulated 2.9-, 6.2-, 7.4-, 2.0-, and 2.2-fold, respectively.

We chose *SPL3*, *SPL9*, and *SPL10* as representative members to investigate whether their expression patterns were disrupted in *hyl1-2* seedlings. In wild-type seedlings, the expression of *SPL3*, *SPL9*, and *SPL10* increased over time from d 7 to 19 (Fig. 6A). In *hyl1-2* seedlings, *SPL3* expression was much higher than in the wild type and increased progressively with time, showing an inverse relationship to miR156. Similar expression profiles were observed for *SPL9* and *SPL10*, although the differences between the expression pattern of the miRNAs and its target genes were not the same as for *SPL3*. To address whether the miR156-targeted genes were downregulated in *hyl1-2 p35S::miR156a* plants, we examined the expression levels of *SPL3*, *SPL9*, and *SPL10* in 10-d-old seedlings by real-time PCR. Expression of the three *SPL* genes decreased in *hyl1-2 p35S::miR156a* seedlings relative to *hyl1-2* and wild-type plants (Fig. 6B). We wondered whether HYL1 controlled the other miR156-targeted *SPL* genes. Real-time PCR revealed that the expression levels of *SPL2*, *SPL4*, *SPL5*, *SPL6*, *SPL11*, *SPL13*, and *SPL15* were elevated in *hyl1-2* to different extents, but expression levels of each in *hyl1-2 35S::miR156a* plants were reduced, except for *SPL4*, whose expression level was slightly higher than that of the wild type (see Supplementary Fig. S1, available in *JXB* online), suggesting that all of the miR156-targeted *SPL* genes were under the control of HYL1. The primary leaves of *hyl1-2 p35S::miR156a* seedlings became juvenile (Fig. 2A), apparently because the expression levels of the *SPL* genes in *hyl1-2 p35S::miR156a* seedlings were below the threshold required for the adult phase. We suggest that HYL1 controls the juvenile state of primary leaves through temporal regulation of miR156-targeted genes.

Single loss-of-function mutants of *SPL3* and *SPL10* show no obvious vegetative phenotype. In contrast, *spl9-4* showed a slight juvenile epidermal phenotype, while an *spl9-4 spl15-1* double mutant exhibited a delayed transition from the juvenile to the adult phase (Wu and Poethig, 2006; Wang *et al.*, 2008; Wu *et al.*, 2009). To address genetic interactions between the miR156-targeted *SPL* genes and HYL1, we constructed *hyl1-2 spl9-4 spl15-1* triple mutants by crossing *hyl1-2* plants with *spl9-4 spl15-1* plants (Fig. 5C, D, F). The triple mutants significantly delayed abaxial trichome production compared with *hyl1-2* single mutants but advanced abaxial trichome production compared with wild-type plants (Fig. 2A). In other words, the *hyl1-2* phenotype was partially rescued by the *spl9-4 spl15-1* alleles. Although the leaves of *hyl1-2 spl9-4 spl15-1* plants were as round as the wild-type leaves, their initiation rates were not significantly increased (Fig. 2B).

The *p35S::rSPL3* (miR156-resistant version of *SPL3*) plants showed early induction of flowering, but there was no significant effect on leaf shape. However, overexpression of *SPL9* and *SPL10* accelerated the expression of all adult leaf traits (Wang *et al.*, 2008; Wu *et al.*, 2009). We generated plants transgenic for *p35S::rSPL3*, *pSPL9::rSPL9* and *pSPL10::rSPL10*, among which the *rSPL9* plants were more similar to the *hyl1-2* plants in the shape of the leaf and petiole (Fig. 2A). To define the genetic interaction between *SPL* genes and HYL1, we introduced *rSPL9* into *hyl1-2* mutants (Fig. 5H, I). In *hyl1-2 pSPL9::rSPL9* plants, all of the primary leaves generated abaxial trichomes, and the number of abaxial trichomes present on the first two leaves was increased compared with that of the *hyl1-2* mutants (Fig. 2A); the leaf initiation rate was also higher than that of *hyl1-2* or *pSPL9::rSPL9* plants (Fig. 2B), suggesting that the adult characteristics of the first leaves were enhanced.

Table 2. miRNA-targeted genes upregulated >1.5-fold in 3-week-old *hyl1* seedlings relative to the wild type

Accession no.[a]	Gene	miRNAs	Fold change
AT1G72830	*HAP2C*	miR169a, -b, -c, -h, -i, -j, -k, -l, -m, -n	12.197156
AT5G06510	*CBF-B/NF-YA*	miR169b, -c, -d, -e, -f, -g, -h, -i, -j, -k, -l, -m, -n	9.1556805
AT3G15270	*SPL5*	miR156a, -b, -c, -d, -e, -f, -g; miR157d	7.4200788
AT3G05690	*HAP2B*	miR169b, -c, -d, -e, -f, -g, -h, -i, -j, -k, -l, -m, -n	7.0425992
AT1G53160	*SPL4*	miR156a, -b, -c, -d, -e, -f, -g, -h; miR157a, -b, -c, -d	6.1503794
AT1g52070	*JR/MBP*	miR846a	5.352703
AT1G63150	*PPR*	miR161.1a, miR161.2a	4.8119594
AT3G57230	*AGL16*	miR824a	4.7594344
AT2G02850	*ARPN*	miR408a	4.6092139
AT1G01040	*DCL1*	miR162a, -b	4.462162
AT1g52060	*JR/MBP*	miR846a	4.0534713
AT1G17590	*rCBF-B/NF-YA*	miR169a, -b, -c, -h, -i, -j, -k, -l, -m, -n	3.8572252
AT1G31280	*AGO2*	miR403a	3.7480951
AT1G63130	*PPR*	miR161.1a; miR400a	3.0100167
AT1G30490	*PHV*	miR165a, -b; miR166a, -b, -c, -d, -e, -f, -g	3.0088157
AT3G11440	*ATMYB65*	miR159c	2.9420524
AT2G33810	*SPL3*	miR156a, -b, -c, -d, -e, -f, -g	2.9262585
AT1G63080	*PPR*	miR161.1a; miR400a	2.8489617
AT5G06100	*MYB33*	miR159c	2.6038222
AT3G09220	*LAC7*	miR857a	2.5730044
AT1G12290	*CC-NBS-LRR*	miR472a	2.5651874
AT3G15030	*TCP4*	miR319a, -b, -c	2.4187059
AT1G54160	*CBF-B/NF-YA*	miR169a, -b, -c, -h, -i, -j, -k, -l, -m, -n	2.3524761
AT1G27370	*SPL10*	miR156a, -b, -c, -d, -e, -f, -g, -h; miR157a, -b, -c, -d	2.2149103
AT3G20910	*CBF-B/NF-YA*	miR169a, -b, -c, -d, -e, -f, -g	2.0370432
AT3G60630	*SCARECROW*	miR170a; miR171a, -b, -c	2.0144381
AT2G42200	*SPL9*	miR156a, -b, -c, -d, -e, -f, -g, -h; miR157a, -b, -c, -d	1.9632046
AT1G56010	*NAC1*	miR164a, -b, -c	1.9609002
AT1G52150	*ATHB-15*	miR165a, -b; miR166a, -b, -c, -d, -e, -f, -g	1.9513054
AT1G77850	*ARF17*	miR160a, -b, -c	1.8860873
AT5G60690	*REV*	miR165a, -b; miR166a, -b, -c, -d, -e, -f, -g	1.7754512
AT1G53230	*TCP3*	miR319a, -b, -c	1.7221409
AT4G30080	*ARF16*	miR160a, -b, -c	1.6402834
AT5G43780	*APS4*	miR395a, -b, -c, -d, -e, -f	1.5858944
AT1G76810	*eIF-2*	miR771a	1.5199657

[a] The Arabidopsis Information Resource database: http://www.arabidopsis.org/.

Blade base angle is a new morphological marker for the juvenile-to-adult-phase transition

During further phenotyping of *hyl1-2* and wild-type leaves, we observed that the blade base angle (BBA; the angle formed by a common endpoint in the base that is shared by the petiole and blade) of wild-type leaves varied among developmental stages. In primary leaves, the BBA was nearly 90° (Fig. 7A), consistent with what is generally observed for round leaves. The BBA increased from the third to the tenth leaves, consistent with gradual elongation of the leaves. The BBA for the 13th leaves was 135°, whereas that of the third leaves was 107°, demonstrating a distinction between the juvenile and adult phases. Therefore, we designated BBA as a new quantitative marker for the juvenile or adult phase. In *hyl1-2* mutants, the BBA values for the third and 13th leaves were almost the same (142°), and both were greater than those of wild-type plants, indicating that the third leaves of *hyl1-2* plants displayed the same characteristics as the adult leaves of both *hyl1-2* and wild-type plants (Fig. 7B). In *hyl1-2 p35S::miR156a* plants, the BBA of the third leaves was the same as that of the wild type, and the BBA of the 13th leaves was 110°, which was much lower than that of *hyl1-2* and wild-type adult leaves. These results implied that, when *p35S::miR156a* recovers juvenile characteristics of the third leaves from the *hyl1-2* phenotype, it enables the 13th adult leaves to acquire juvenile characteristics.

In *hyl1-2 spl9-4 spl15-1* plants, the BBA of the third leaves was lower than that of *hyl1-2* but higher than that of the wild-type (Fig. 7B), while the BBA of the 13th leaves was lower than that of *hyl1-2* and the wild-type but higher than that of *spl9-4 spl15-1* plants. These results indicated that the adult characteristic of both the third and 13th leaves was compromised in *hyl1-2 spl9-4 spl15-1* plants.

The transgenic *p35S::miR156a* plants exhibited a much stronger rescue of the *hyl1-2* mutant phenotype than was seen in *spl9-4 spl15-1* plants. The limited restoration of *spl9-4 spl15-1* alleles to the *hyl1-2* phenotype indicated that HYL1 regulates other *SPL* genes besides *SPL9* and *SPL15*.

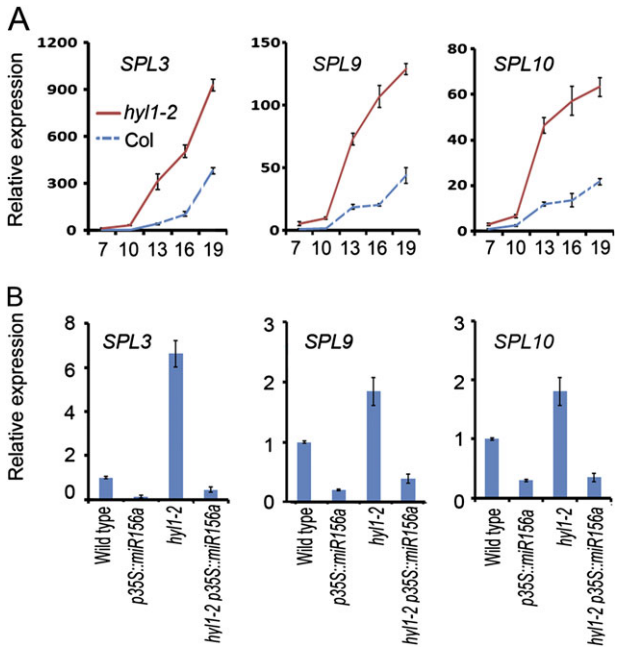

Fig. 6. Expression of *SPL3*, *SPL9*, and *SPL10* genes in *hyl1-2* and transgenic plants. (A) Progressive expression levels of miR156-targeted *SPL3*, *SPL9*, and *SPL10* genes in wild-type and *hyl1-2* seedlings from 7 to 19 d after germination (DAG; *x*-axis) Total RNA was extracted from the shoot apex at different stages and analysed by real-time RT-PCR with three biological replicates. Expression was normalized relative to that of the wild type at 7 DAG. (B) Expression of *SPL3*, *SPL9*, and *SPL10* genes in wild-type, *hyl1-2*, *p35S::miR156a*, and *hyl1-2 p35S::miR156a* 10-d-old seedlings. Three biological replicates were performed. Results are shown as means ±SD.

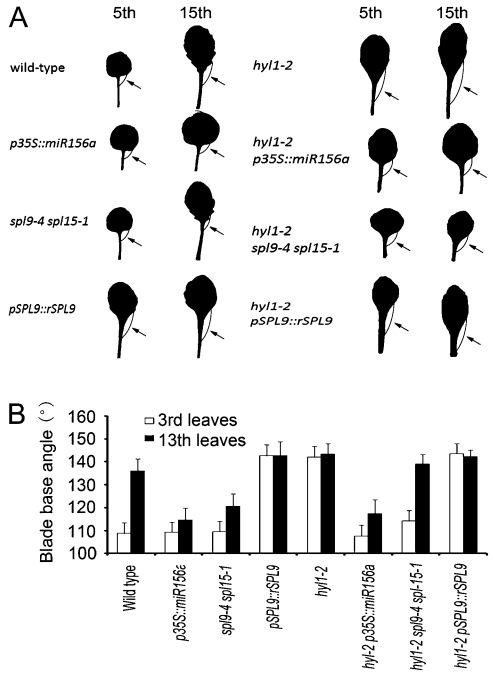

Fig. 7. Blade base angles (BBA) of 50-d-old seedling of *hyl1-2* and related mutants grown under short-day conditions. (A) Circular arcs in the fifth and 15th leaves indicate the BBA (arrows). (B) Comparison of BBA among *hyl1-2* and related mutants. The number of leaves measured was >30. Results are shown as means ±SD.

In all of these cases, high BBA values (>140°) for the leaves were correlated with the presence of abaxial trichomes and an elongated blade, while low BBA values (<120°) were correlated with an absence of abaxial trichomes and round blades. In summary, high BBA, the presence of abaxial trichomes on primary leaves, and a high length-to-width ratio of blades are three useful morphological markers to distinguish between adult and juvenile leaves.

HYL1 controls crosstalk between miR156 and miR165/166

hyl1-2 plants are characterized by leaf incurvature, which is attributable to adaxial–abaxial polarity defects due to reduced accumulation of miR165/166 (Yu *et al.*, 2005). In *Arabidopsis*, five of the class III homeodomain-leucine zipper (HD-ZIP III) genes are targeted by miR165/166. Of these, *PHABULOSA* (*PHB*), *PHAVOLUTA* (*PHV*), and *REVOLUTA* (*REV*) act redundantly to promote the adaxial cell fates of the leaf primordium (McConnell and Barton, 1998; McConnell *et al.*, 2001; Emery *et al.*, 2003), while *ATHB8* (*HB-8*) and *CORONA* (*CNA*) encode functions that are both antagonistic to those of *REV* within certain tissues and overlap those of *REV* in other tissues (Emery *et al.*, 2003). In *hyl1-2 p35S::miR156a* and *hyl1-2 spl9-4 spl15-1* plants, the complete rescue of the *hyl1-2* phenotype in terms of early phase transition was concurrent with a reduction in leaf incurvature (Fig 5B–F), revealing that increased accumulation of miR156 or loss of function of the *SPL* genes contributed to the partial recovery from leaf incurvature. Our previous report confirmed that deficiency in the miR165/166 pathways was the primary cause for leaf incurvature of *hyl1* mutants (Liu *et al.*, 2011). To address the relationship between miR156 and miR165/166 or miR165/166-targeted genes, the accumulation of miR165/166 and miR165/166-targeted genes in *hyl1-2 p35S::miR156a* and *hyl1-2 pSPL9::rSPL9* plants was analysed. The amount of miR165/166 decreased in plants transgenic for *p35S::miR156a*, whereas in those transgenic for *pSPL9::rSPL9* it increased (Fig. 4C). To test whether *SPL9* regulated miR165/166-targeted genes, we examined the expression level of HD-ZIP III genes using real-time PCR. Transcripts of *REV* were elevated about 2-fold in *pSPL9::rSPL9* plants and decreased slightly in *p35S::miR156a* plants (Fig. 4D). In *hyl1-2* plants, the expression of *REV*, *PHB*, and *PHV* increased in *hyl1-2 pSPL9::rSPL9* plants but decreased in *hyl1-2 p35S::miR156a* plants (Fig. 4D). These results suggested that overaccumulation of miR156a or reduced expression of *SPL* genes downregulated the expression of some HD-ZIP III genes. Loss-of-function mutations of *REV*, *PHB*, and *PHV* rescue the incurvature phenotype of *hyl1* leaves (Liu *et al.*, 2011),

which is why the extent of leaf incurvature decreased in *hyl1-2 p35S::miR156a* plants.

HYL1 prevents the premature transcription of adult-related genes in primary leaves

In *hyl1-2* mutants, the adult characteristics of the primary leaves are consistent with the up- and downregulation of many genes, including miR156-mediated targets. These genes might be responsible for differentiation of the abaxial trichomes, proliferation of the proximo-distal axis, and cell division at the blade base. To examine the premature gene transcripts of adult-related genes, we searched for miR156-regulated genes among the differentially expressed transcripts in *hyl1-2* mutants. These genes could be responsible for the premature gene expression observed in *hyl1-2* primary leaves and might be partially required for functioning of the *SPL* genes. We compared microarray libraries from *hyl1* with those from *hyl1-2 p35S::miR156a* and selected ten genes that were most differentially expressed between *hyl1* and wild-type seedlings, and between *hyl1-2 p35S::miR156a* and *hyl1* seedlings. We chose the three genes (*ENH1*, At1g26920, and *MYB59*) that were downregulated in *hyl1* seedlings relative to the wild type and upregulated in *hyl1-2 p35S::miR156a* seedlings relative to *hyl1* seedlings, and seven genes (*PAP17*, At5g05250, *ORG1*, *FRO3*, At1g47400, *SPL3*, and *SPL5*) that were upregulated in *hyl1* seedlings relative to the wild type and downregulated in *hyl1-2 p35S::miR156a* seedlings relative to *hyl1* seedlings (see Supplementary Table S1, available in *JXB* online).

To define the genes regulated by HYL1 through miR156-mediated *SPL* genes, we examined the premature expression of the differentially expressed genes by real-time PCR. In the primary leaves of 10-d-old seedlings (juvenile phase), the three downregulated genes exhibited decreased transcript levels in *hyl1-2* plants relative to wild-type plants and increased transcription levels in *hyl1-2 p35S::miR156a* plants relative to *hyl1-2* plants (Fig. 8). Four of the five upregulated genes (the exception was *ORG1*) showed increased transcript levels in *hyl1-2* plants relative to the wild type and decreased transcript levels for *hyl1-2 p35S::miR156a* plants relative to *hyl1-2* plants, suggesting that these genes are adult-stimulative. Surprisingly, the *ENH1*, At1g26920, and *MYB59* genes all showed increased transcript levels in the 15th leaves of 50-d-old *hyl1-2* plants relative to their primary leaves. Hence, we concluded that these genes are regulated differently in primary and adult leaves of *hyl1-2* plants. Most of the adult-stimulative genes showed increased transcript levels in the 15th *hyl1-2* leaves relative to *hyl1-2* primary leaves, or in the 15th wild-type leaves relative to primary wild-type leaves. Therefore, they may play an important role in expression of adult traits in both wild-type and *hyl1-2* leaves. These results suggest that HYL1 mediates the expression of adult-related genes that regulate adult-phase development of primary leaves.

As SE, another important regulator of miRNA biogenesis, is involved in the vegetative-phase transition, we

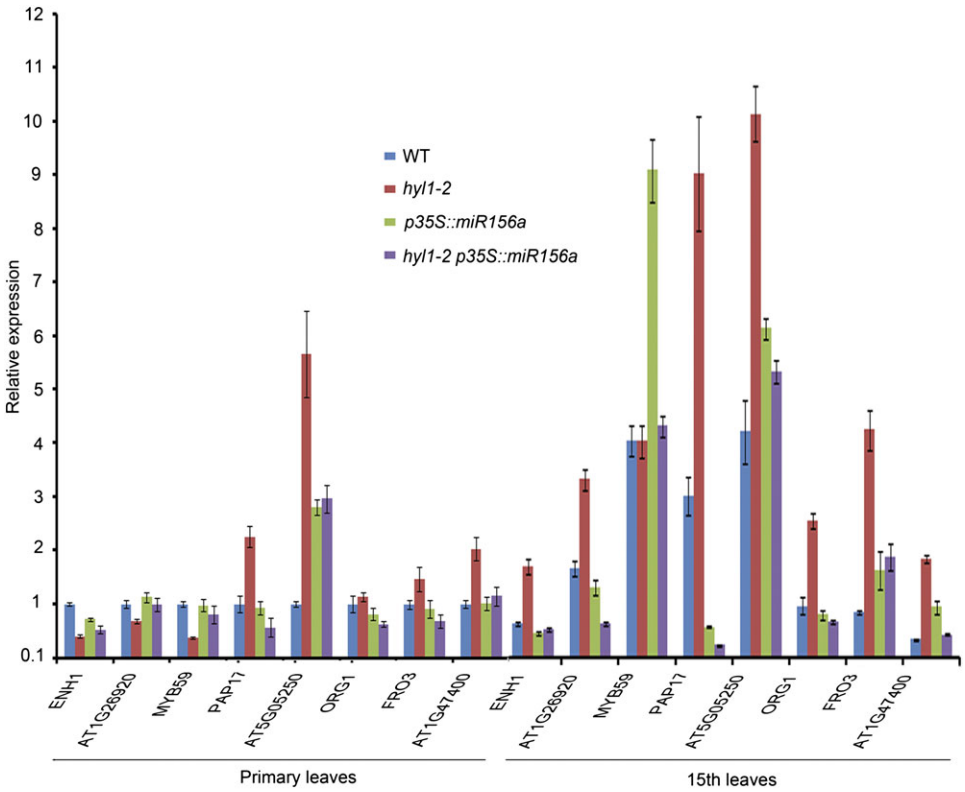

Fig. 8. Premature gene expression in the primary leaves and 15th leaves of *hyl1-2*, *hyl1-2 p35S::miR156a*, and the wild-type (WT). Three biological replicates were performed. Results are shown as means ±SD.

wondered whether *hyl1* and *se-1* mutants would exhibit similar premature gene expression patterns. To address this question, we examined the ten genes expressed most differentially between *se-1* plants and the wild type, and between *se-1 p35S::miR156f* (miR156f is the same as miR156a) and *se-1* seedlings using data described previously (Wang *et al.*, 2008). Among these, six genes, including *SPL3*, were the most upregulated in *se-1* seedlings relative to the wild type and downregulated in *se-1 p35S::miR156f* relative to *se-1* seedlings. We observed that *SPL5* was not downregulated in *se-1 p35S::miR156f*. A comparison of the genes most differentially expressed between *se-1* and *se-1 p35S::miR156f* revealed that all of the most downregulated genes in *hyl1 p35S::miR156a* seedlings (see Supplementary Table S2, available in *JXB* online) were also downregulated in *se-1 p35S::miR156f* seedlings. In contrast, two of the most upregulated genes in *se-1* seedlings were also upregulated in *hyl1* seedlings. The premature expression of some *SPL*-regulated genes was clearly shared in *hyl1* and *se-1* seedlings. However, many of these genes were not common in *hyl1* and *se-1* seedlings. We wondered whether these genes were upregulated in *hyl1-2* plants relative to wild-type primary leaves, and whether they were preferentially expressed in the 15th leaves of *hyl1-2* mutants compared with the primary leaves. Compared with the control gene sets, the genes showing at least a 2-fold increase in their transcript levels in *hyl1-2* primary leaves were significantly enriched in the 15th leaves relative to the primary leaves.

Discussion

HYL1 supplies abundant miR156 for the juvenilization of primary leaves

The periods of vegetative growth of higher plants vary with species, genotypes, and environmental conditions (Wang *et al.*, 2011). In tomato and cucumber, vegetative growth and reproductive growth are intertwined throughout life, and pure vegetative growth is very short. In contrast, many *Brassica* crops such as Chinese cabbage and cabbage undergo vegetative growth in natural conditions for long period (>5 months). For example, the vegetative growth of Chinese cabbage is divided into four stages: seedling, rosette, folding, and heading (He *et al.*, 2000), each of which is characterized by timing of abaxial trichomes, blade shape, and petiole length. A seedling stage is necessary for the formation of nutrient-rich heads. In *Arabidopsis*, the juvenile phase (equivalent to the seedling stage of Chinese cabbage) can be subdivided into the early juvenile phase and late juvenile phase. Normally, miR156a accumulates throughout vegetative growth, but it peaks during the early juvenile phase and decreases progressively during the subsequent vegetative phases with time. HYL1 controls the relative high accumulation of miR156a in primary leaves that is essential for the juvenile state, as it is preferentially expressed in the same regions where miR156a accumulates. In *hyl1-2* mutants, a lack of *HYL1* results in reduced accumulation of miR156 and in turn enhanced expression of miR156-targeted *SPL* genes compared with the wild type. During vegetative growth, reduced accumulation of miR156a causes an adult-like phenotype in the primary leaves and early transition of the adult phase in the first nine leaves. In this case, juvenile-to-adult-phase transition is determined by temporal expression of pri-miR156 and *HYL1* genes. HYL1 must supply an abundance of miR156 for the juvenilization of primary leaves.

In *hyl1-2 p35S::miR156a* or *hyl1-2 spl9-4 spl15-1* plants, the *hyl1-2* phenotype in terms of abaxial trichome placement on primary leaves, elongation of the blade, and the increase in the BBA were completely or partially rescued. In *hyl1-2 pSPL9::rSPL9* plants, the *hyl1-2* phenotype was altered by the increased early appearance of abaxial trichomes, enhanced elongation of the blade, and an increased BBA. These observations revealed that HYL1 determines the timing of the juvenile-to-adult-phase transition through an miR156-mediated pathway.

HYL1 and SE might control different SPL*-regulated genes*

The genes that mediate the effects of the miR156-targeted *SPL* genes during leaf development are unknown. These *SPL* genes might exhibit similar functions to adaxial–abaxial identity genes, cell division genes, and auxin response factors that regulate the differentiation of abaxial trichomes, elongation of the blade and increases in the BBA. How HYL1 organizes these genes through miRNA-mediated *SPL* genes is not clear. In other aspects, the gain-of-function mutation of *iaa18* or *axr3-1*, two members of the Aux/IAA transcriptional repressor family, has pleiotropic phenotypes, including long hypocotyls and up-curled leaves (Leyser *et al.*, 1996; Cline *et al.*, 2001; Uehara *et al.*, 2008; Ploense *et al.*, 2009). These phenotypes are similar to those of the *hyl1-2* plants. It would be interesting to explore whether these genes were involved in HYL1-regulated developmental processes.

In *Arabidopsis*, the presence of trichomes on the abaxial surface of the leaf is often used as a morphological marker for the adult phase. The number of serrations, trichomes, and hydathodes, the size of the petiole and leaf blade, the length-to-width ratio of the leaf blade, and vascular complexity are also used to investigate vegetative-phase transition (Telfer *et al.*, 1997; Tsukaya *et al.*, 2000; Usami *et al.*, 2009). In this study, we used the BBA as a new marker for analysis of phase transition. In general, differentiation of morphological markers, such as serrations, trichomes, hydathodes, petioles, blades, the length-to-width ratio of the leaf blade, and the BBA, is established by patterns of cell division that are often highly variable.

HYL1 defines the timing of abaxial trichome appearance, leaf shape, and BBA. However, the marginal serrations of the *hyl1-2* leaves are not obvious, and the number of hydathodes was not changed compared with wild-type leaves. These results indicate that HYL1 regulates trichome patterns, the length-to-width ratio of the leaf blade, and the

BBA, rather than serrations and hydathodes. In contrast, SE determines the timing of abaxial trichome, serration, and hydathode appearance. In theory, the *SPL*-regulated genes regulate leaf shape and BBA, while a different set of *SPL*-regulated genes determines serration and hydathodes.

SPL3 and *SPL5* belong to the same class of the miR156-mediated *SPL* gene family. Both genes are downregulated in *hyl1-2 p35S::miR156a* relative to *hyl1-2* seedlings, while *SPL3* alone is downregulated in *se-1 p35S::miR156f* relative to *se-1* seedlings. It remains unclear whether these subtle differences alter the premature expression of *SPL*-regulated genes. Nevertheless, not all of the genes that are most differentially expressed between *hyl1-2 p35S::miR156a* and *se-1 p35S::miR156f* are the same. This suggests that the premature gene expression in the primary leaves of *hyl1-2* is not the same as for *se-1*. We suggest that HYL1 and SE might regulate different *SPL*-regulated genes and control different morphological traits.

Supplementary data

Supplementary data are available at *JXB* online.

Supplementary Table S1. The ten genes that were most deregulated (upregulated and downregulated) in *hyl1* seedlings relative to the wild type and in *hyl1-2 p35S::miR156a* (*hyl1 156*) relative to *hyl1* seedlings.

Supplementary Table S2. The ten genes that were most deregulated (upregulated and downregulated) in *se-1* seedlings relative to the wild type and *se-1 p35S::miR156a* relative to *se-1* seedlings. The data were derived from GEO GSE16061.

Supplementary Table S3. Oligonucleotide primer sequences used in this study.

Supplementary Fig. S1. Expression of *SPL2*, *SPL4*, *SPL5*, *SPL6*, *SPL11*, *SPL1I3*, and *SPL15* genes in *hyl1-2* and transgenic plants. Expression was normalized relative to that of the wild type and are shown as means ±SD.

Acknowledgements

We are grateful to Dr R. Scott Poethig for providing *spl9-4 spl15-1* seeds and plasmids *pSPL9::rSPL9* and *pSPL10::rSPL10* and to Dr Detlef Weigel for providing plasmid *p35S::rSPL3*. This work was supported by grants from the Natural Science Foundation of China (grant no. 30730053) and National Basic Research Program of China (grant no. 2012CB113903).

References

Chuck G, Cigan AM, Saeteurn K, Hake S. 2007. The heterochronic maize mutant *Corngrass1* results from overexpression of a tandem microRNA. *Nature Genetics* **39,** 544–549.

Clarke JH, Tack DT, Findlay K, Van Montagu M, Van Lijsebettens M. 1999. The *SERRATE* locus controls the formation of the early juvenile leaves and phase length in *Arabidopsis*. *The Plant Journal* **20,** 493–501.

Cline MG, Chatfield SP, Leyser O. 2001. NAA restores apical dominance in the *axr3-1* mutant of *Arabidopsis thaliana*. *Annals of Botany* **87,** 61–65.

Clough SJ, Bent AF. 1998. Floral dip: a simplified method for *Agrobacterium*-mediated transformation of *Arabidopsis thaliana*. *The Plant Journal* **16,** 735–743.

Dong Z, Han MH, Fedoroff N. 2008. The RNA-binding proteins HYL1 and SE promote accurate *in vitro* processing of pri-miRNA by DCL1. *Proceedings of the National Academy of Sciences USA* **105,** 9970–9975.

Emery JF, Floyd SK, Alvarez J, Eshed Y, Hawker NP, Izhaki A, Baum SF, Bowman JL. 2003. Radial patterning of *Arabidopsis* shoots by class IIIHD-ZIP and KANADI genes. *Current Biology* **13,** 1768–1774.

Fang YD, Spector DL. 2007. Identification of nuclear dicing bodies containing proteins for microRNA biogenesis in living *Arabidopsis* plants. *Current Biology* **17,** 818–823.

Fujioka Y, Utsumi M, Ohba Y, Watanabe Y. 2007. Location of a possible miRNA processing site in SmD3/SmB nuclear bodies in *Arabidopsis*. *Plant and Cell Physiology* **48,** 1243–1253.

Guo AY, Zhu QH, Gu X, Ge S, Yang J, Luo J. 2008. Genome-wide identification and evolutionary analysis of the plant specific SBP-box transcription factor family. *Gene* **418,** 1–8.

Han MH, Goud S, Song L, Fedoroff N. 2004. The *Arabidopsis* double-stranded RNA-binding protein HYL1 plays a role in microRNA-mediated gene regulation. *Proceedings of the National Academy of Sciences USA* **101,** 1093–1098.

He YK, Xue WX, Sun YD, Yu XH, Liu PL. 2000. Leafy head formation of the progenies of transgenic plants of Chinese cabbage with exogenous auxin genes. *Cell Research* **10,** 151–160.

Hiraguri A, Itoh R, Kondo N, Nomura Y, Aizawa D, Murai Y, Koiwa H, Seki M, Shinozaki K, Fukuhara T. 2005. Specific interactions between Dicer-like proteins and HYL1/DRB-family dsRNA-binding proteins in *Arabidopsis thaliana*. *Plant Molecular Biology* **57,** 173–188.

Kurihara Y, Kaminuma E, Matsui A, *et al*. 2009. Transcriptome analyses revealed diverse expression changes in *ago1* and *hyl1 Arabidopsis* mutants. *Plant and Cell Physiology* **50,** 1715–1720.

Kurihara Y, Takashi Y, Watanabe Y. 2006. The interaction between DCL1 and HYL1 is important for efficient and precise processing of pri-miRNA in plant microRNA biogenesis. *RNA* **12,** 206–212.

Leyser HM O, Pickett FB, Dharmasiri S, Estelle M. 1996. Mutations in the *AXR3* gene of *Arabidopsis* result in altered auxin response including ectopic expression from the *SAUR-AC1* promoter. *The Plant Journal* **10,** 403–413.

Liu Z, Jia L, Wang H, He Y. 2011. HYL1 regulates the balance between adaxial and abaxial identity for leaf flattening via miRNA-mediated pathways. *Journal of Experimental Botany* **62,** 4367–4381.

Lobbes D, Rallapalli G, Schmidt DD, Martin C, Clarke J. 2006. SERRATE: a new player on the plant microRNA scene. *EMBO Reports* **7,** 1052–1058.

Lu C, Fedoroff N. 2000. A mutation in the *Arabidopsis HYL1* gene encoding a dsRNA binding protein affects responses to abscisic acid, auxin, and cytokinin. *Plant Cell* **12,** 2351–2365.

Machida S, Chen HY, Yuan YA. 2011. Molecular insights into miRNA processing by *Arabidopsis thaliana* SERRATE. *Nucleic Acids Research* **39,** 7828–7836.

McConnell JR, Barton MK. 1998. Leaf polarity and meristem formation in *Arabidopsis*. *Development* **125,** 2935–2942.

McConnell JR, Emery J, Eshed Y, Bao N, Bowman J, Barton MK. 2001. Role of *PHABULOSA* and *PHAVOLUTA* in determining radial patterning in shoots. *Nature* **411,** 709–713.

Ploense SE, Wu MF, Nagpal P, Reed JW. 2009. A gain-of-function mutation in IAA18 alters *Arabidopsis* embryonic apical patterning. *Development* **136,** 1509–1517.

Shikata M, Koyama T, Mitsuda N, Ohme-Takagi M. 2009. *Arabidopsis* SBP-box genes SPL10, SPL11 and SPL2 control morphological change in association with shoot maturation in the reproductive phase. *Plant and Cell Physiology* **50,** 2133–2145.

Song L, Han MH, Lesicka J, Fedoroff N. 2007. *Arabidopsis* primary microRNA processing proteins HYL1 and DCL1 define a nuclear body distinct from the Cajal body. *Proceedings of the National Academy of Sciences USA* **104,** 5437–5442.

Telfer A, Bollman KM, Poethig RS. 1997. Phase change and the regulation of trichome distribution in *Arabidopsis thaliana*. *Development* **124,** 645–654.

Tsukaya H, Shoda K, Kim GT, Uchimiya H. 2000. Heteroblasty in *Arabidopsis thaliana* (L.) Heynh. *Planta* **210,** 536–542.

Uehara T, Okushima Y, Mimura T, Tasaka M, Fukaki H. 2008. Domain II mutations in CRANE/IAA18 suppress lateral root formation and affect shoot development in *Arabidopsis thaliana*. *Plant and Cell Physiology* **49,** 1025–1038.

Usami T, Horiguchi G, Yano S, Tsukaya H. 2009. The more and smaller cells mutants of *Arabidopsis thaliana* identify novel roles for *SQUAMOSA PROMOTER BINDING PROTEIN-LIKE* genes in the control of heteroblasty. *Development* **136,** 955–64.

Vazquez F, Gasciolli V, Crete P, Vaucheret H. 2004. The nuclear dsRNA binding protein HYL1 is required for microRNA accumulation and plant development, but not posttranscriptional transgene silencing. *Current Biology* **14,** 346–351.

Wang JW, Czech B, Weigel D. 2009. miR156-regulated SPL transcription factors define an endogenous flowering pathway in *Arabidopsis thaliana*. *Cell* **138,** 738–749.

Wang JW, Park MY, Wang LJ, Koo Y, Chen XY, Weigel D, Poethig RS. 2011. miRNA control of vegetative phase change in trees. *PLoS Genet* 7, e1002012.

Wang JW, Schwab R, Czech B, Mica E, Weigel D. 2008. Dual effects of miR156-targeted *SPL* genes and *CYP78A5/KLUH* on plastochron length and organ size in *Arabidopsis thaliana*. *Plant Cell* **20,** 1231–43.

Weigel D, Glazebrook J. 2006. In planta transformation of Arabidopsis. *Cold Spring Harbor Protocols* doi:10.1101/pdb.prot4668.

Willmann MR, Poethig RS. 2005. Time to grow up: the temporal role of smallRNAs in plants. *Current Opinion in Plant Biology* **8,** 548–52.

Willmann MR, Poethig RS. 2011. The effect of the floral repressor FLC on the timing and progression of vegetative phase change in *Arabidopsis*. *Development* **138,** 677–85.

Wu G, Park MY, Conway SR, Wang JW, Weigel D, Poethig RS. 2009. The sequential action of miR156 and miR172 regulates developmental timing in *Arabidopsis*. *Cell* **138,** 750–759.

Wu G, Poethig RS. 2006. Temporal regulation of shoot development in *Arabidopsis thaliana* by *miR156* and its target *SPL3*. *Development* **133,** 3539–3547.

Yang L, Liu ZQ, Lu F, Dong AW, Huang H. 2006. SERRATE is a novel nuclear regulator in primary microRNA processing in *Arabidopsis*. *Plant Journal* **47,** 841–850.

Yang SW, Chen HY, Yang J, Machida S, Chua NH, Yuan YA. 2010. Structure of *Arabidopsis* HYPONASTIC LEAVES1 and its molecular implications for miRNA processing. *Structure* **18,** 594–605.

Yu L, Yu X, Shen R, He Y. 2005. *HYL1* gene maintains venation and polarity of leaves. *Planta* **221,** 231–242.